AGU PUBLICATIONS

Water Resources Research

RESEARCH ARTICLE
10.1002/2013WR014668

Impact of losing and gaining streamflow conditions on hyporheic exchange fluxes induced by dune-shaped bed forms

Aryeh Fox[1], Fulvio Boano[2], and Shai Arnon[1]

[1]Department of Environmental Hydrology and Microbiology, Zuckerberg Institute for Water Research, The Jacob Blaustein Institutes for Desert Research, Ben-Gurion University of the Negev, Sede Boqer, Israel, [2]Department of Environment, Land and Infrastructure Engineering, Politecnico di Torino, Turin, Italy

Key Points:
- Hyporheic exchange fluxes under losing and gaining conditions were measured
- Hyporheic exchange flux decreases when the losing and gaining flux increases
- Coupling between streamflow and regional gradient controls hyporheic exchange

Correspondence to:
S. Arnon,
sarnon@bgumail.ac.il

Citation:
Fox, A., F. Boano, and S. Arnon (2014), Impact of losing and gaining streamflow conditions on hyporheic exchange fluxes induced by dune-shaped bed forms, *Water Resour. Res.*, *50*, 1895–1907, doi:10.1002/2013WR014668.

Received 29 AUG 2013
Accepted 21 JAN 2014
Accepted article online 24 JAN 2014
Published online 6 MAR 2014

Abstract The exchange of water between the surface and subsurface environments plays a crucial role in hydrological, biogeochemical, and ecological processes. The exchange of water is driven by the local morphology of the streambed (hyporheic exchange) and the regional forcing of a large-scale hydraulic gradient, which results in losing or gaining flow conditions. We measured the effects of losing and gaining flow conditions on hyporheic exchange fluxes in a sandy streambed using a novel laboratory flume system (640 cm long and 30 cm wide) under a combination of average overlying velocities and losing/gaining fluxes. Hyporheic exchange fluxes were analyzed based on a new conceptual framework. This combination of experimental observations and modeling revealed that hyporheic exchange fluxes under losing and gaining flow conditions are similar. Because interfacial transport increases proportionally to the square of the overlying velocity and linearly with increasing fluxes of losing and gaining conditions in the sand bed, the hyporheic exchange flux becomes smaller when the losing or gaining flux increases. Thus, losing and gaining flow conditions become the dominant mechanisms of water exchange at a certain flux, which depends on the competitive interaction between the overlying velocity in the stream and the losing/gaining fluxes.

1. Introduction

Interactions between stream and groundwater systems have been considered by many studies to play a fundamental role in contaminant transport and remediation, in the functioning of aquatic ecosystems, and in water resources management [*Sophocleous*, 2002; *Boulton et al*., 2010; *Hester and Gooseff*, 2010; *Krause et al*., 2013]. Further, the interactions between the stream and the streambed induce water fluxes into and out of the channel bed and banks (i.e., the hyporheic zone), which are commonly termed hyporheic exchange flows [*Findlay*, 1995]. The intensity and the direction of the exchange between streams and subsurface water may follow complex patterns at multiple scales that depend mainly on the hydrologic conditions in both the stream and the groundwater (e.g., water levels), the sediment permeability, and the morphology of the sediment surrounding the stream channel [*Dent et al*., 2007; *Ruehl et al*., 2007; *Buffington and Tonina*, 2009; *Cardenas*, 2009]. For example, hyporheic flow is driven by dune-shaped bed forms [*Elliott and Brooks*, 1997a; *Packman et al*., 2004], pool-riffle sequences [*Bencala and Walters*, 1983; *Tonina and Buffington*, 2007], meander point bars [*Boano et al*., 2006; *Cardenas*, 2009], and regional groundwater flows induced by the large-scale topography of the catchment [*Wörman et al*., 2007].

The scientific literature on surface-subsurface interactions includes many studies that rely on experiments and observations at field or laboratory scales, such as indoor flumes [*Elliott and Brooks*, 1997a; *Marion et al*., 2002; *Salehin et al*., 2004]. Most experimental field studies have been aimed at evaluating the magnitude and direction of the water exchange [*Kasahara and Wondzell*, 2003; *Peterson and Sickbert*, 2006; *Gariglio et al*., 2013]. Studies of this kind provide valuable information on the behavior of the hydrological system, and on hyporheic exchange, but they are often limited for predictive purposes due to their dependence on the specific characteristics of the study sites, which hinders generalizing the research findings. Modeling studies, on the other hand, have significantly contributed to understanding how physical principles control hyporheic exchange. In some cases, modeling efforts were also validated against experimental data [*Elliott and Brooks*, 1997a; *Marion et al*., 2002; *Salehin et al*., 2004; *Tonina and Buffington*, 2007]. However, the

systematic effects of gaining and losing flow conditions on hyporheic exchange have only been shown in modeling studies [*Cardenas and Wilson*, 2007a, 2007b; *Boano et al*., 2008, 2009b; *Trauth et al*., 2013].

There is an increasing body of evidence showing that solute exchange and biogeochemical reactions closely depend on hyporheic exchange and on residence time in the subsurface [*Zarnetske et al*., 2011; *Bardini et al*., 2012; *Gomez et al*., 2012; *Marzadri et al*., 2012; *Arnon et al*., 2013]. It has also been shown that losing and gaining fluxes control the size of the hyporheic zone, in addition to the primary imposed direction of the main fluxes [*Gariglio et al*., 2013; *Voltz et al*., 2013]. Thus, the interactions between local hyporheic exchange and losing or gaining fluxes are expected to be complex and lead to different sizes and shapes of the biogeochemical active zone. However, there were no affirmations of these modeling results by experimental data due to the difficulties involved in controlling the hydrological conditions in experimental systems. Currently, a comprehensive, validated quantitative framework for the estimation of the rates of hyporheic water fluxes under different gaining/losing conditions is still missing, and it is this lack of a quantitative framework that is addressed in this study. We postulated that hyporheic exchange fluxes will decrease under losing and gaining streamflow conditions in a similar manner, and this was evaluated by (1) quantifying how losing and gaining streamflow conditions influence hyporheic exchange fluxes of water and solutes in a novel laboratory flume that enables the control on losing and gaining conditions and (2) developing a new framework for calculating stream-subsurface water fluxes and solute exchange.

2. Materials and Methods

2.1. Experimental Setup

The stream-subsurface exchange of solutes was studied using a 640 cm long and 29 cm wide recirculating flume (Figure 1). The flow in the flume was driven by a centrifugal pump, and the discharge was measured with a magnetic flowmeter placed in the return pipe (SITRANS F mag 5000, Siemens). The flume bottom had no slope, and under the flow conditions used in the experiments, there were no significant differences in the water depth along the channel due to the very small water surface slope.

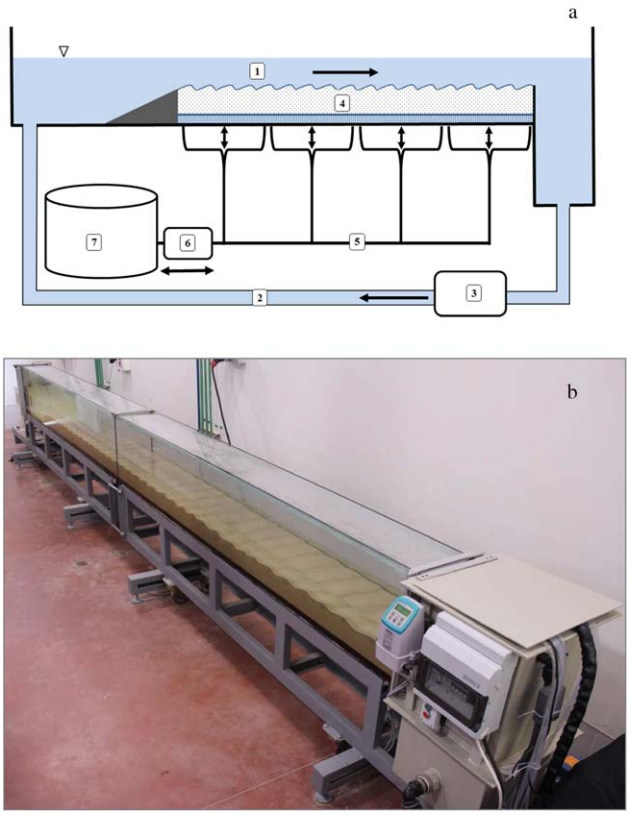

Figure 1. (a) Schematic illustration and (b) a picture of the experimental setup. The numbers show the main channel (1), the circulation pipe (2), the centrifugal pump for driving the flow in the channel (3), the sand bed (4), the drainage/injection system (5), the four-channel peristaltic pump for imposing losing or gaining flow conditions (6), and the reservoir for storing injected or withdrawn water from the flume (7).

The flume was packed with natural silica sand having an average diameter of 384 μm, a porosity of 0.33 that was measured using the water evaporation method, and a hydraulic conductivity of 0.1195 cm s^{-1} assessed using the constant head method [*Klute and Dirksen*, 1986]. The sand was arranged in dune-shaped bed forms—structures of 15 cm in length and 2 cm in height. The bed form height and wavelength did not vary along the width of the flume. Average water depth was measured from the water surface to the mean bed level and was 7 cm, while the sediment thickness was 11 cm.

The dimensions of the bed forms that were used in this study are commonly found in sandy streambeds [e.g., *Stofleth et al.*, 2008; *Lewandowski et al.*, 2011; *Harvey et al.*, 2013]. Those dimensions typically vary within the range of bed form lengths of 10–25 cm, bed form height of 1–4 cm, and water depth of 5–40 cm. Bed form dimension varies mainly according to the flow velocity and sediment characteristics, and are independent of the water depth. Interestingly, constant scaling was observed between bed form height and length over 5 orders of magnitude [*Ashley*, 1990].

To enforce losing or gaining flow conditions in the sand bed, a drainage system was constructed at the bottom of the flume. The drainage system was made from 128 evenly distributed single pumping points, arranged in a network that drained the flume bottom from four separated sections. Each section had an area of 0.39 m^2, from which water could be pumped in or out of the system, using a four-channel peristaltic pump (Master Flex model 7523-80, Cole Parmer).

2.2. Evaluating the Ability of the Drainage System to Produce Uniform Flow in the Sand Bed

A tracer experiment was conducted under losing conditions in order to evaluate the uniformity of the flow in the sand bed by injecting a nonreactive tracer (190 g of NaCl) into the overlying water. The overlying water velocity in the main channel was maintained at 12.3 cm s^{-1}. Water was pumped from the four different subsections of the drainage system at a total flow rate of 24 L d^{-1}, which resulted in a water flux per unit bed area of 9.1 cm d^{-1}, while the same amount of water that was pumped through the drainage system was added to the surface water to maintain the water depth and overlying velocity constant. Electrical Conductivity (EC) was measured and logged every 5 min in the main channel and at the four outlets of the drainage system by using CS547A-LEC sensors and a CR1000 data logger (Campbell Scientific). This experiment was conducted before and after the measurements of surface-subsurface exchange (section 2.3) to ensure that the drainage system function did not change over the course of the experiments.

2.3. Surface-Subsurface Exchange

Hyporheic exchange flux was measured with tracer experiments under various combinations of two overlying water velocities, 4.3 and 12.3 cm s^{-1}, and six subsurface flow rates. Re numbers ($Re = V \cdot 4r/\nu$) for the 4.3 and 12.3 cm s^{-1} were 1.2×10^4 and 3.4×10^4, respectively. Re was calculated following *García* [2008], where V is the mean velocity of the overlying flow (cm s^{-1}), r is a characteristic length (cm) defined here as the hydraulic radius (i.e., water depth), and ν is the kinematic viscosity of the fluid (cm^2 s^{-1}). The aforementioned range of water velocities is typically found in streams with sandy streambeds and similar values are commonly used in flume studies [e.g., *Strommer and Smock*, 1989; *Mutz*, 2000, 2003; *Ren and Packman*, 2004; *Hünken and Mutz*, 2007; *Wörman et al.*, 2007; *Stofleth et al.*, 2008; *Harvey et al.*, 2012; *Janssen et al.*, 2012; *Kessler et al.*, 2012]. Subsurface flow rates vary from fluxes of 63 cm d^{-1} to no flow conditions (neutral conditions). These are well within the ranges of velocities measured in streams with sandy streambeds, although data on this topic are not frequently reported in the literature [e.g., *Engelhardt et al.*, 2011; *Lewandowski et al.*, 2011; *Bhaskar et al.*, 2012].

Tracer experiments were conducted by introducing a tracer solution to the recirculating water, and then monitoring the reduction in the in-stream tracer concentration over time [*Packman et al.*, 2004]. Dissolved NaCl was used as a conservative tracer, and its concentration was measured as EC using an LR 925/01 electrode connected to a multi 3430 logger (WTW). The background EC in the flume was approximately 90 and 160 μS cm^{-1}, before and after the tracer addition, respectively. The resolution of the sensor was 0.1 μS cm^{-1}. Changes in tracer concentrations were sufficiently small to avoid fluxes induced by density gradients [*Boano et al.*, 2009b; *Jin et al.*, 2011]. Water temperature was maintained at 25 ± 1°C.

Losing and gaining flow conditions were imposed by controlling the flow rate and direction through the drainage system using a peristaltic pump, as described in section 2.1. Under losing conditions, water was pumped downward through the sand and out of the flume, while under gaining conditions, water was injected through the sand into the main channel. In order to maintain a constant water volume, water depth, and overlying water velocity in the flume, water with a known EC was added to the channel or pumped out of the main channel, under losing and gaining flow conditions, respectively. Hyporheic exchange fluxes under different flow conditions were calculated based on the rate of change in the EC in the main channel using the analytical framework described in section 3.

The rates of decline of the hyporheic fluxes under different losing or gaining flow rates were compared by fitting the observed data with an exponential decay equation. Then, the independent fit was compared to

the fit of a combined data set that shared data from both curves. We compared the sum-of-squares of each independent fit and the combined fit using the extra sum-of-squares *F* test in the statistical software GraphPad Prism (version 5).

Dye injections were also used to visualize the rates and extent of surface-subsurface exchange. Twenty-five grams of the dye Brilliant Blue FCF was added to the channel, and the penetration of the dye was recorded by sequential photographs taken every 1 min through the flume's glass walls. All the dye additions were performed at an overlying water velocity of 12.3 cm s^{-1}. One dye addition was performed without imposing losing or gaining flow conditions (i.e., neutral conditions). Other dye injections were performed by imposing losing and gaining conditions of water flux per unit bed area of 18 and 49 cm d^{-1} (Figure 1).

Images from all the experiments were analyzed for the dye distribution in the sand bed, using a self-made routine for batch image analysis, performed with the C programming language. The routine included a threshold adjustment for RGB colors (bulk water, sand bed, and the dye), and the calculation of pixel area coverage for each color.

3. Analytical Development and Modeling

3.1. Hyporheic Flux Calculation

The presence of groundwater inflow or outflow through the streambed was not considered in previous laboratory studies [*Marion et al*., 2002; *Packman et al*., 2004; *Boano et al*., 2009a], and a mathematical framework to quantify hyporheic fluxes in gaining or losing conditions is currently not available. In order to achieve the research objectives, a method was developed to evaluate the water flux per streambed area, q_H, which will be denoted as hyporheic flux for the sake of brevity. This flux indicated the water exchange flux that flows from the overlying water to the sand bed and returns back to the overlying water after a period of time.

The mass balance equations for a nonreactive tracer were presented by *Boano et al*. [2009a] for the case of neutral conditions. When a net loss of water is present, the equations become:

$$W\frac{dC}{dt} = A[q_H(C_s - C) + q_L C_{out} - q_L C] \tag{1}$$

$$W_s\frac{dC_s}{dt} = A[-q_H(C_s - C) - q_L C_s + q_L C] \tag{2}$$

$$C(t=0) = C_0 \tag{3}$$

$$C_s(t=0) = 0 \tag{4}$$

where t is time after full mixing of the injected tracer in surface water, W is the total volume of surface water (including water tanks and pipes), W_s is the pore water volume, $C(t)$ and $C_s(t)$ are the average tracer concentrations in surface water and pore water, respectively, A is the streambed area, q_L is the imposed losing flux per unit bed area, and C_{out} is the concentration in the replacement water that is added to the flume to avoid altering the total water volume. The term $q_L C_{out}$ in equation (1) accounts for the progressive dilution of surface water caused by the addition of the replacement solution.

By assuming that the concentration within sediments is negligible ($C_s \approx 0$) during the initial part of each experiment [e.g., *Grant et al*., 2012], the evolution of in-stream concentration is simply given by:

$$\frac{dC}{dt} = -\frac{q_H + q_L}{d}C + \frac{q_L}{d}C_{out} \tag{5}$$

where $d = W/A$ represents the equivalent depth of surface water. The solution of equations (5) and (3) is:

$$C(t) = C_0\exp\left[-\frac{q_H + q_L}{d}t\right] + \frac{q_L}{q_H + q_L}C_{out}\left(1 - \exp\left[-\frac{q_H + q_L}{d}t\right]\right) \tag{6}$$

which, at short times after the tracer injection ($t << d/(q_H + q_L)$), can also be simplified into

$$C^*(t) = \frac{C(t)}{C_0} = 1 - \frac{q_H + q_L}{d} t + C^*_{out} \frac{q_L}{d} t \tag{7}$$

where $C^*_{out} = C_{out}/C_0$. The q_H can be calculated from the (negative) slope S of the initial stage of the $C^*(t)$ curve, which, from equation (7), can be expressed as

$$S = \frac{dC^*}{dt} = -\frac{q_H + q_L}{d} + \frac{q_L}{d} C^*_{out} \tag{8}$$

which can be rearranged to derive the desired expression for q_H under losing conditions:

$$q_H = -q_L \left(1 - C^*_{out}\right) - S\ d \tag{9}$$

A different way to classify the different exchange components is to discriminate between the downward flux q_{down} that flows from the stream to the sediments and the upward flux q_{up} that flows through the streambed surface in the opposite direction. As depicted in the previous figure, hyporheic exchange induced by bed topography contributes to both q_{down} and q_{up}, while the losing flux only contributes to q_{down}. In losing conditions, it is therefore possible to define

$$q_{down} = q_H + q_L \tag{10}$$

$$q_{up} = q_H \tag{11}$$

The approach for gaining flow conditions is similar to the one for the losing conditions. The different flow configuration leads to the mass balance equations:

$$W \frac{dC}{dt} = A[q_H(C_s - C) + q_G C_s - q_G C] \tag{12}$$

$$W_s \frac{dC_s}{dt} = A[q_H(C - C_s) - q_G C_s + q_G C_{out}] \tag{13}$$

where q_G is the imposed gaining flux. Again, at times sufficiently close to the tracer injection, we can neglect the tracer concentration in the sediments compared to that in the surface water, thus obtaining

$$\frac{dC}{dt} = -\frac{q_H + q_G}{d} C \tag{14}$$

whose solution is

$$C(t) = C_0 \exp\left[-\frac{q_H + q_G}{d} t\right] \approx C_0 \left(1 - \frac{q_H + q_G}{d} t\right) \tag{15}$$

where the last approximate equality holds for ($t << d/(q_H + q_G)$). The next step is to define the dimensionless in-stream concentration $C^*(t) = C(t)/C_0$ and then calculate its slope from equation (15) as

$$S = \frac{dC^*}{dt} = -\frac{q_H + q_G}{d} \tag{16}$$

which eventually leads to the final expression

$$q_H = -q_G - S\ d \tag{17}$$

Finally, the downward and upward fluxes can be written as

$$q_{down} = q_H \tag{18}$$

$$q_{up} = q_H + q_G \tag{19}$$

In neutral conditions, there is neither a losing nor gaining flux from the flume bottom (i.e., $q_L = q_G = 0$), and both equations (9) and (17) reduce to

$$q = -S\ d \tag{20}$$

3.2. Predictive Theory for Hyporheic Exchange

Here we briefly summarize the theory proposed by *Boano et al*. [2009b] to determine how hyporheic exchange is altered by groundwater inflow to a gaining stream. The method is based on the theory presented by *Elliott and Brooks* [1997b], according to which the hyporheic exchange flux in neutral conditions, $q_{H,0}$, can be evaluated as:

$$q_{H,0} = \frac{K\ k\ h_0}{\pi} = \frac{2\ K\ h_0}{L} \tag{21}$$

where K is the streambed hydraulic conductivity, $k = 2\pi/L$ is the bed form wave number, L is the bed form wavelength, and h_0 is the amplitude of the hydraulic head profile along the bed form. This head difference was related to the properties of the streamflow by the following expression:

$$h_0 = a\frac{U^2}{2g}\left(\frac{H/d_S}{0.34}\right)^m \tag{22}$$

where a is a dimensionless coefficient, U is the stream velocity, H is the bed form height, d_S is the stream depth, g is the gravity acceleration, and the exponent m is equal to 3/8 if $H < 0.34\ d_S$ and 3/2 otherwise. The coefficient a depends on the bed form shape (steepness, asymmetry), and the average value $a = 0.28$ was proposed by *Elliott and Brooks* [1997b] from a meta analysis of a number of laboratory experiments with different bed form shapes.

Equation (21) was extended by *Boano et al*. [2009b] to consider the case of a stream receiving a net groundwater inflow. The main result of the inclusion of an ambient groundwater inflow q_G is given by the following predictive equations for the hyporheic exchange flux q_H and the total flux $q_T = q_H + q_G$:

$$q_H = q_{H,0}\sqrt{1-\left(\frac{1}{\pi}\frac{q_G}{q_{H,0}}\right)^2} + \frac{q_G}{\pi}\arcsin\left(\frac{1}{\pi}\frac{q_G}{q_{H,0}}\right) - \frac{q_G}{2} \tag{23}$$

$$q_T = q_{H,0}\sqrt{1-\left(\frac{1}{\pi}\frac{q_G}{q_{H,0}}\right)^2} + \frac{q_G}{\pi}\arcsin\left(\frac{1}{\pi}\frac{q_G}{q_{H,0}}\right) + \frac{q_G}{2} \tag{24}$$

The total flux q_T represents the overall flux of water that reaches the streamflow through the streambed interface (see Figure 2) and coincides with the upward flux defined by equation (19).

The case of a losing stream can be easily recovered from the previous analysis by taking advantage of the symmetrical structure of the Laplace equation which governs water flow in the sediments. It can be shown that equations (23) and (24) can still be applied to calculate the hyporheic and total fluxes by simply replacing q_G with the losing flux q_L. In the case of a net groundwater loss from the stream, the total flux q_T represents the overall flux of water from the stream to the sediments as in equation (10).

4. Results and Discussion

A tracer experiment was used to verify the ability of the drainage system to enforce uniform flow conditions within the sand bed in the flume. Breakthrough curves of the salt tracer in the four outlets of the

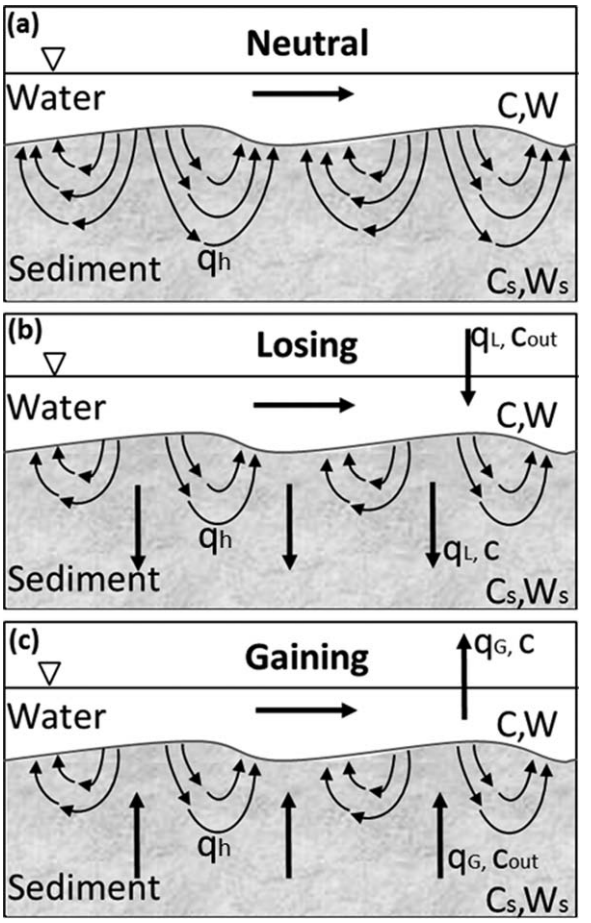

Figure 2. Conceptual illustration of flow patterns and model notation under (a) neutral conditions, (b) losing conditions, and (c) gaining conditions.

subsections of the drainage system were not considerably different (Figure 3). The first arrival times of the tracer in sections 1 and 4 (155 and 145 min, respectively) were slightly earlier than those in sections 2 and 3 (220 and 180 min, respectively). The earlier arrival times in sections 1 and 4 were probably influenced by the proximity of these sections to the edges of the sand bed, adjacent to the inlet and outlet sections of the flume, where lateral transport toward the edges was restricted. The differences between the four subsections diminished relatively quick, and the travel time for the center of mass ($C/C_0 = 0.5$) was similar for all subsections (373 ± 6 min).

Hyporheic exchange flux, q_H, was measured in a series of experiments under different flow conditions. As noted in section 3.1, q_H refers to the water that initially travels from the stream into the subsurface porous medium, but returns after some time to the surface water. In the experiments, q_H decreased exponentially with increasing losing or gaining fluxes, q_L and q_G, respectively (Figure 4). q_H was suppressed at a q_L or q_G of about 12 and 48 cm d^{-1}, for overlying flow velocities of 4.3 and 12.3 cm s^{-1}, respectively. A fit with an exponential decay equation to the data of an overlying velocity of 12.3 cm s^{-1} under losing and gaining conditions was $y = 14.3\ e^{-0.039x}$ ($R^2 = 0.97$) and $y = 14\ e^{-0.04x}$ ($R^2 = 0.78$), respectively (Figure 4). These exponential fits were not significantly different ($p < 0.01$). The data for q_H under an overlying velocity of 4.3 cm s^{-1} declined to about zero very quickly.

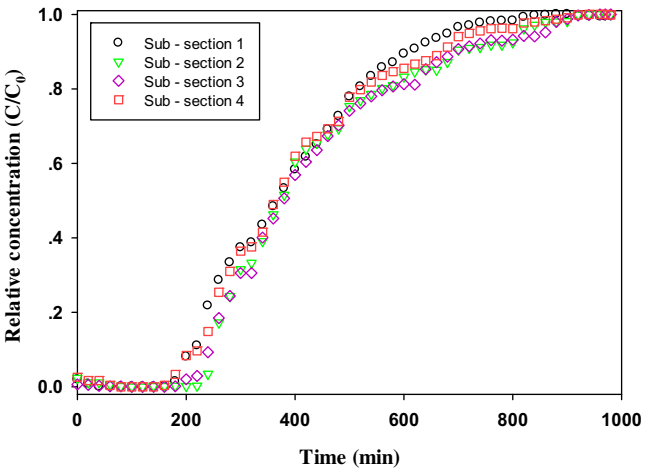

Figure 3. Breakthrough curves of EC as an indicator for chloride transport under losing conditions in the four subsections of the drainage system. The numbers indicate the locations of the subsections along the flume, where 1 is adjacent to the inlet and 4 is close to the outlet.

Model predictions of hyporheic exchange using equations (21–23) were used to fit the experimental data (Figure 4). However, while *Elliott and Brooks* [1997b] considered $a = 0.28$ in

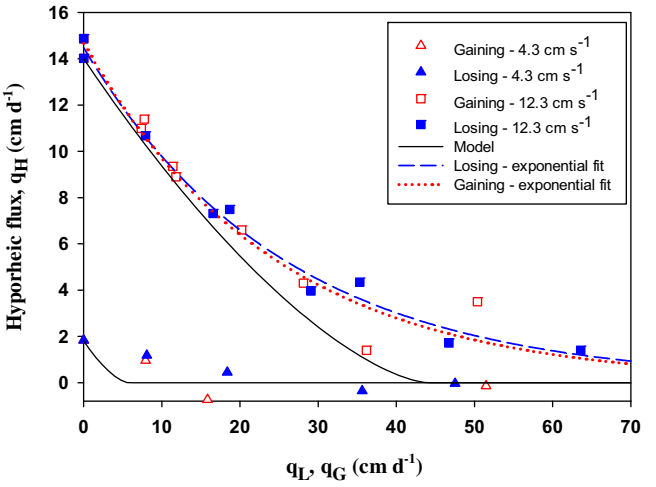

Figure 4. Measured and modeled hyporheic exchange fluxes under various losing and gaining flow conditions, and under overlying water velocities of 4.3 cm s^{-1} and 12.3 cm s^{-1}. Hyporheic flux solely represents the water exchange flux that flows from the overlying water to the sand bed and returns back to the overlying water after a period of time. Neutral conditions are shown as qL or qG = 0.

their model (equation (22)), we used $a = 0.16$ after the calibration of hyporheic exchange flux under neutral conditions. The need for another value for the coefficient a depends on the differences in the bed form shape (length/height ratio, crest position) between our experiments and those considered by *Elliott and Brooks* [1997b]. Even though the value of the exchange flux in neutral conditions was calibrated, the model results exhibit the same trend of decreasing exchange flux with increasing qL or qG that was observed in the experiments (Figure 4). Model predictions also imply that there will be no difference in hyporheic exchange fluxes between the losing and gaining conditions, as seen in the experimental results. Under an overlying velocity of 12.3 cm s^{-1}, the model and the experimental data agree very well for q_L or $q_G < 29$ cm d^{-1}. However, the model slightly underestimates the experimental data at higher q_L or q_G values.

The exponential decrease of q_H with increasing q_L or q_G was also shown by *Cardenas and Wilson* [2007b] and *Trauth et al.* [2013] in a modeling study. Since hyporheic exchange increases proportionally to the square of the overlying velocity [*Packman et al.*, 2004], q_H was suppressed at much higher q_L and q_G values when the overlying velocity was 12.3 cm s^{-1} as compared to an overlying velocity of 4.3 cm s^{-1} (Figure 4). The level at which q_H is suppressed is a result of the competitive interaction between the flow in the stream and the losing/gaining magnitude, and it was shown to be influenced by the Re number or pressure gradients [*Cardenas and Wilson*, 2007a], and is highly influenced by bed form morphology [*Trauth et al.*, 2013]. As the overlying stream velocity decrease (Re number and pressure gradients decreases as well), q_H becomes less significant. For the overlying velocities up to 12.3 cm s^{-1}, losing and gaining fluxes becomes the controlling factor at a q_L or q_G value of 36 cm d^{-1}, thus influencing the total fluxes in the system (see Figure 5 and also q_{down} and q_{up} as described in section 3.1).

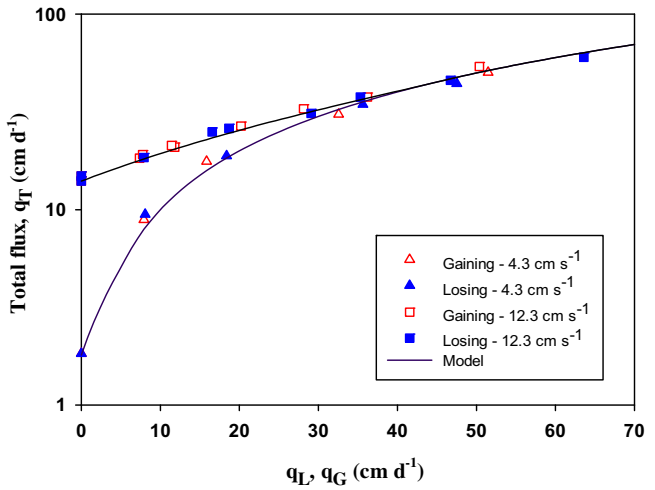

Figure 5. Measured and modeled total flux (see section 3.1.) under various losing and gaining flow conditions. Neutral conditions are shown as qL or qG = 0.

Whereas q_H remained approximately the same magnitude under both losing and gaining conditions, the downwelling flux going from the stream to the subsurface obviously differs between the losing and the gaining conditions. Under gaining conditions, this flux is solely depicted by q_H, while under losing conditions, it is composed of the sum of q_H and the imposed q_L, which reflects the larger-scale/regional control on stream-subsurface exchange [*Boano et al.*, 2009b]. As the imposed flux increases, q_H

decreases and the downwelling becomes more dependent on the imposed flux. The overall impact of neutral, losing, and gaining conditions on the downwelling flux is displayed as a sequence of photographs of a dye tracer penetration to the sand bed (Figure 6). As expected, the downwelling flux of water, as depicted by the dye solute transport, is smallest under gaining conditions, intermediate under neutral conditions, and maximum under losing conditions. Translating the images to the area of the dye coverage (plotted as relative to the whole area of the sand bed) further exemplifies the rate of downwelling flux. The fastest rate of penetration was found for the highest losing flux, while the lowest one was found under the highest gaining flux (Figure 7). While the entire sand bed is expected to be eventually covered by the dye under losing conditions, the area of hyporheic exchange under neutral conditions was still increasing at a very low rate after 270 min, when it was covering 40% of the sediment area. The relative area under gaining conditions reached its final values of 5.5% and 17%, for q_G of 2.05 and 0.76 cm s^{-1}, respectively. Under the high gaining flux, the hyporheic zone was already at its final size after 70 min.

The experimental results clearly show that q_H values under losing and gaining flow conditions were similar (Figure 4), and to the best of our knowledge, this is the first time that clear experimental evidence for this behavior is shown. *Boano et al*. [2008, 2009b] and *Cardenas and Wilson* [2007a, 2007b] showed in modeling studies that the spatial extent of the hyporheic zone is reduced by the upwelling water as compared to neutral conditions. The size of the hyporheic zone was also reduced under losing conditions as predicted by *Cardenas and Wilson* [2007a] and *Cardenas* [2009]. In the losing conditions, the reduction in size of the hyporheic zone occurs due to the transition of streamlines that used to return to the surface toward the downwelling direction. While the overall area, flux, and residence time were similar for the losing and gaining conditions, the spatial distributions of the hyporheic exchange zone and the 3-D flow paths were shown to be markedly different [*Cardenas and Wilson*, 2007a; *Trauth et al*., 2013]. In addition, *Trauth et al*. [2013] specifically demonstrated that while the overall effects of losing and gaining fluxes on hyporheic exchange are similar, under various morphological-hydrodynamic conditions, they are not identical. While our experimental data show that the behavior of q_H is in good agreement with the aforementioned models,

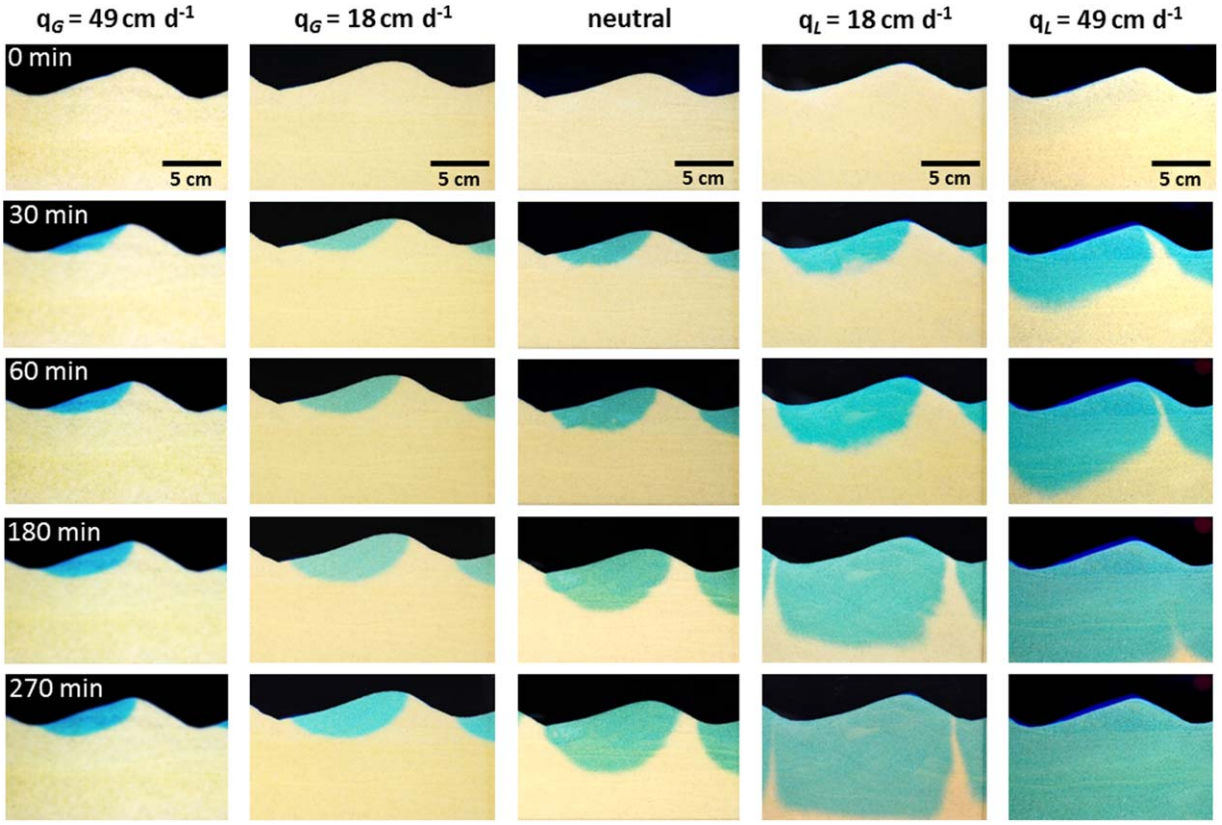

Figure 6. Time series photographs of dye penetration into the sand bed under neutral, losing, and gaining conditions. Flow was from left to right at an overlying water velocity of 12.3 cm s^{-1}.

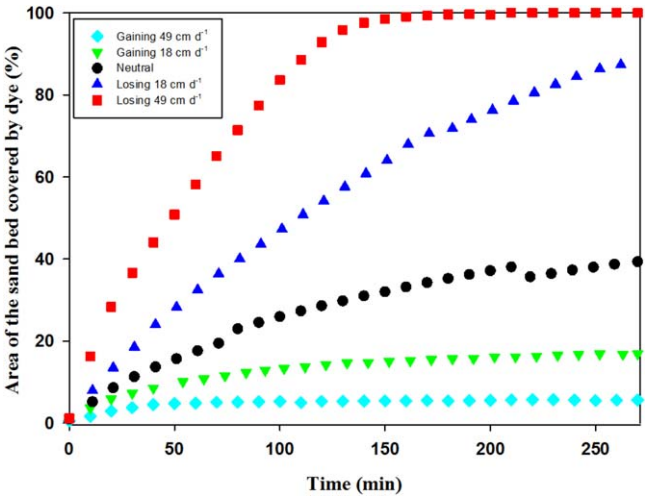

Figure 7. Rate of dye penetration is shown by the relative sand bed area covered by the dye under neutral, losing, and gaining flow conditions versus time. Data extracted from images such as those shown in Figure 6.

the region that q_H occupies cannot be fully resolved with the dye tracer additions, since under losing conditions, the area occupied by the dye is a combination of q_H and q_L.

Accurate quantification of water exchange with the hyporheic zone is a delicate step that is highly dependent on the choices made in the parameterization of the system dynamics [*O'Connor and Harvey*, 2008; *Grant et al.*, 2012]. In this work, we developed a novel modeling framework that allows us to analyze the observed values of surface water concentrations by separating the effect of the imposed losing/gaining flux from the hyporheic exchange flux. When water is injected or abstracted from a flume to reproduce the hydrologic conditions of gaining or losing stream reaches, the signature of hyporheic exchange on surface water concentration is partially obscured by the dilution due to the losing/gaining water flux. The influence of dilution on calculated fluxes helps to explain the differences between observed data and model predictions at high rates of losing/gaining influx (Figure 4). The processes and the flow patterns shown in the results are particularly relevant to streams with sandy streambeds, but potentially transferable also to other type of streambed sediments. While it is expected that q_H will decrease with increasing losing and gaining fluxes in all type of sediments, the magnitude of this change cannot be predicted for different stream systems based on the results from the present flume experiments. This is because the complexity of the streambed morphology and sediment structures at all scales, which is not included in our experiments, is also expected to influence stream-subsurface exchange in general, and hyporheic exchange in particular [*Wörman et al.*, 2007; *Stonedahl et al.*, 2010].

The unique location of the hyporheic zone has the potential to play a key role in many ecological and biogeochemical processes that affect the stream and the groundwater quality, as was previously shown in various studies [*Boano et al.*, 2010; *Zarnetske et al.*, 2011; *Gomez et al.*, 2012; *Mendoza-Lera and Mutz*, 2013]. Under gaining conditions, upwelling groundwater mixes with stream water in the hyporheic zone, and then emerges into the stream. Under losing conditions, downwelling stream water flows through the hyporheic zone toward the groundwater, but some of the downwelling water returns to the stream. In both upwelling and downwelling cases, the mixture of stream and groundwater in the upper layer of the subsurface creates sharp chemical gradients that drive biogeochemical processes. Therefore, the physical flow paths, the residence times, and the region where hyporheic exchange takes place, are all expected to influence biogeochemical processes. While biogeochemical processes require the exchange of solutes between the stream and the subsurface, their effect on stream water quality should be strongly influenced by the relative amount of stream discharge that is exchanged with hyporheic sediments. However, the aforementioned aspect was commonly overlooked as was shown by *Wondzell* [2011] who demonstrated that the ratio between stream discharge and exchange flux per unit stream length, which represents the distance required for the entire water flow in the stream to be exchanged with the subsurface, is mostly significant only in small streams at low discharge. Simple calculations for our flume experiments under neutral conditions resulted in a distances of 6.1 and 16.5 Km, for overlying velocities of 12.3 and 4.3 cm s^{-1}, respectively. However, as was mentioned before, the relatively simplified experimental configuration cannot capture many additional processes that are influencing solute exchange at different scales (e.g., moving bed forms or different morphological structures such as bed forms, meanders, etc.) as was shown in other studies [e.g., *Stonedahl et al.*, 2010; *Harvey et al.*, 2012].

The findings of this research stress the importance of the complex coupled interaction between the flow conditions in the stream and in the subsurface, which effectively defines the active region of the hyporheic zone, in particular, and the flow patterns in the subsurface, in general (Figures 6 and 7), as is also illustrated by other recent studies [e.g., *Bardini et al*., 2012; *Marzadri et al*., 2012; *Trauth et al*., 2013]. It was previously shown that changes in hyporheic exchange due to overlying velocity alone could lead to a complex nonlinear response in denitrification activity [*Arnon et al*., 2007; *O'Connor and Hondzo*, 2008] due to the changes in the redox conditions. This type of interaction could be magnified or eliminated by incorporating losing or gaining flow conditions (Figure 4) and a residence time distribution analysis to extents that have only recently become an active topic of modeling research with very limited experimental data [*Bardini et al*., 2012; *Kessler et al*., 2012].

5. Conclusions

Hyporheic exchange flux is driven by local and regional-scale geomorphological structures and hydraulic gradients in a complex manner. The relative importance of turbulence, bed form structures, and regional-scale hydraulic gradients has been a topic of many studies in the last decades. In this study, we evaluate how losing and gaining streamflow conditions influence hyporheic exchange fluxes induced by dune-shaped bed forms using a novel laboratory flume, and we develop a new framework for calculating stream-subsurface water fluxes. It was found that hyporheic exchange flux becomes smaller than the exchange under neutral conditions when the losing or gaining fluxes increase. The rate of decline in hyporheic exchange flux was exponential, and was statistically similar under both losing and gaining flow conditions. Losing and gaining flow conditions become the dominant mechanisms of water exchange at a threshold flux, which depends on the competitive interaction between the overlying velocity in the stream and the losing/gaining fluxes. While this study showed a simple case of interaction between small geomorphic structures and losing and gaining fluxes, further study is needed in order to evaluate how hyporheic exchange fluxes driven by larger structures, such as meander bends and riffles interact with regional groundwater [e.g., *Cardenas*, 2009b; *Trauth et al*., 2013].

A novel modeling framework was developed that enabled analyzing the observed values of surface water concentrations by separating the effect of the imposed losing/gaining flux from the hyporheic exchange flux. The model framework allows us to evaluate the influence of dilution on the calculated fluxes under gaining conditions, and the effect of downwelling flow on water and solute transport toward the groundwater. The coupling between stream velocity and losing/gaining flow conditions is expected to regulate nutrient and contaminant transport, and should be incorporated into regional-scale modeling frameworks that describe solute transport in streams.

Acknowledgments

This research was supported by the Israel Science Foundation (grant 694/11) to S. Arnon, and by a grant (Israel-Italy Joint Innovation Program for Scientific and Technological Cooperation in R&D) from the Israeli Ministry of Science, Technology and Space and the Italian Ministry of Foreign Affairs, Directorate General for Political and Security Affairs to S. Arnon and F. Boano. We thank Nadège de Chambrier for assistance with the image analysis. We also thank two anonymous reviewers, Susa Stonedahl, and Associate Editor Steve Wondzell for providing constructive comments that greatly improved this paper.

References

Arnon, S., K. A. Gray, and A. I. Packman (2007), Biophysicochemical process coupling controls nitrate use by benthic biofilms, *Limnol. Oceanogr.*, *52*(4), 1665–1671.

Arnon, S., K. Yanuka, and A. Nejidat (2013), Impact of overlying water velocity on ammonium uptake by benthic biofilms, *Hydrol. Processes*, *27*(4), 570–578, doi:10.1002/hyp.9239.

Ashley, G. M. (1990), Classification of large-scale subaqueous bedforms; A new look at an old problem, *J. Sediment.*, *1*(60), 160–172, doi: 10.2110/jsr.60.160.

Bardini, L., F. Boano, M. B. Cardenas, R. Revelli, and L. Ridolfi (2012), Nutrient cycling in bedform induced hyporheic zones, *Geochim. Cosmochim. Acta*, *84*, 47–61, doi:10.1016/j.gca.2012.01.025.

Bencala, K. E., and R. A. Walters (1983), Simulation of solute transport in a mountain pool-and-riffle stream: a transient storage model, *Water Resour. Res.*, *19*(3), 718–724.

Bhaskar, A. S., J. W. Harvey, and E. J. Henry (2012), Resolving hyporheic and groundwater components of streambed water flux using heat as a tracer, *Water Resour. Res.*, *48*, W08524, doi:10.1029/2011WR011784.

Boano, F., C. Camporeale, R. Revelli, and L. Ridolfi (2006), Sinuosity-driven hyporheic exchange in meandering rivers, *Geophys. Res. Lett.*, *33*, L18406, doi:10.1029/2006GL027630.

Boano, F., R. Revelli, and L. Ridolfi (2008), Reduction of the hyporheic zone volume due to the stream-aquifer interaction, *Geophys. Res. Lett.*, *35*, L09401, doi:10.1029/2008GL033554.

Boano, F., R. Revelli, and L. Ridolfi (2009a), Quantifying the impact of groundwater discharge on the surface-subsurface exchange, *Hydrol. Processes*, *2116*, 2108–2116, doi:10.1002/hyp.7278.

Boano, F., D. Poggi, R. Revelli, and L. Ridolfi (2009b), Gravity-driven water exchange between streams and hyporheic zones, *Geophys. Res. Lett.*, *36*, L20402, doi:10.1029/2009GL040147.

Boano, F., A. Demaria, R. Revelli, and L. Ridolfi (2010), Biogeochemical zonation due to intrameander hyporheic flow, *Water Resour. Res.*, *46*, W02511, doi:10.1029/2008WR007583.

Boulton, A. J., T. Datry, T. Kasahara, M. Mutz, and J. A. Stanford (2010), Ecology and management of the hyporheic zone: Stream–groundwater interactions of running waters and their floodplains, *J. N. Am. Benthol. Soc.*, *29*(1), 26–40, doi:10.1899/08–017.1.
Buffington, J. M., and D. Tonina (2009), Hyporheic exchange in mountain rivers II: Effects of channel morphology on mechanics, scales, and rates of exchange, *Geogr. Compass*, *3*(3), 1038–1062, doi:10.1111/j.1749–8198.2009.00225.x.
Cardenas, M. B. (2009), Stream-aquifer interactions and hyporheic exchange in gaining and losing sinuous streams, *Water Resour. Res.*, *45*, W06429, doi:10.1029/2008WR007651.
Cardenas, M. B., and J. L. Wilson (2007a), Exchange across a sediment–water interface with ambient groundwater discharge, *J. Hydrol.*, *346*(3-4), 69–80, doi:10.1016/j.jhydrol.2007.08.019.
Cardenas, M. B., and J. L. Wilson (2007b), Thermal regime of dune-covered sediments under gaining and losing water bodies, *J. Geophys. Res.*, *112*, G04013, doi:10.1029/2007JG000485.
Dent, C. L., N. B. Grimm, E. Marti, J. W. Edmonds, J. C. Henry, and J. R. Welter (2007), Variability in surface-subsurface hydrologic interactions and implications for nutrient retention in an arid-land stream, *J. Geophys. Res.*, *112*, G04004, doi:10.1029/2007JG000467.
Elliott, A. H., and N. H. Brooks (1997a), Transfer of nonsorbing solutes to a streambed with bed forms: Laboratory experiments, *Water Resour. Res.*, *33*(1), 137–151, doi:10.1029/96WR02783.
Elliott, A. H., and N. H. Brooks (1997b), Transfer of nonsorbing solutes to a streambed with bed forms: Theory, *Water Resour. Res.*, *33*(1), 123–136, doi:10.1029/96WR02784.
Engelhardt, I., M. Piepenbrink, N. Trauth, S. Stadler, C. Kludt, M. Schulz, C. Schüth, and T. A. Ternes (2011), Comparison of tracer methods to quantify hydrodynamic exchange within the hyporheic zone, *J. Hydrol.*, *400*(1-2), 255–266, doi:10.1016/j.jhydrol.2011.01.033.
Findlay, S. E. G. (1995), Importance of surface-subsurface exchange in stream ecosystems: The hyporheic zone, *Limnol. Oceanogr.*, *40*(1), 159–164.
García, M. H. (2008), Sediment transport and morphodynamics, in *Sedimentation Engineering*, edited by M. H. García, pp. 21–164, Am. Soc. of Civ. Eng., Reston, Va.
Gariglio, F. P., D. Tonina, and C. H. Luce (2013), Spatiotemporal variability of hyporheic exchange through a pool-riffle-pool sequence, *Water Resour. Res.*, *49*, 7185–7204, doi:10.1002/wrcr.20419.
Gomez, J. D., J. L. Wilson, and M. B. Cardenas (2012), Residence time distributions in sinuosity-driven hyporheic zones and their biogeochemical effects, *Water Resour. Res.*, *48*, W09533, doi:10.1029/2012WR012180.
Grant, S. B., M. J. Stewardson, and I. Marusic (2012), Effective diffusivity and mass flux across the sediment-water interface in streams, *Water Resour. Res.*, *48*, W05548, doi:10.1029/2011WR011148.
Harvey, J. W., et al. (2012), Hydrogeomorphology of the hyporheic zone: Stream solute and fine particle interactions with a dynamic streambed, *J. Geophys. Res.*, *117*, G00N11, doi:10.1029/2012JG002043.
Harvey, J. W., J. K. Böhlke, M. A. Voytek, D. Scott, and C. R. Tobias (2013), Hyporheic zone denitrification: Controls on effective reaction depth and contribution to whole-stream mass balance, *Water Resour. Res.*, *49*, 6298–6316, doi:10.1002/wrcr.20492.
Hester, E. T., and M. N. Gooseff (2010), Moving beyond the banks: Hyporheic restoration is fundamental to restoring ecological services and functions of streams, *Environ. Sci. Technol.*, *44*(5), 1521–1525, doi:10.1021/es902988n.
Hünken, A., and M. Mutz (2007), Field studies on factors affecting very fine and ultra fine particulate organic matter deposition in low-gradient sand-bed streams, *Hydrol. Processes*, *533*(21), 525–533, doi:10.1002/hyp.6263.
Janssen, F., M. B. Cardenas, A. H. Sawyer, T. Dammrich, J. Krietsch, and D. de Beer (2012), A comparative experimental and multiphysics computational fluid dynamics study of coupled surface–subsurface flow in bed forms, *Water Resour. Res.*, *48*, W08514, doi:10.1029/2012WR011982.
Jin, G., H. Tang, L. Li, and D. A. Barry (2011), Hyporheic flow under periodic bed forms influenced by low-density gradients, *Geophys. Res. Lett.*, *38*, L22401, doi:10.1029/2011GL049694.
Kasahara, T., and S. M. Wondzell (2003), Geomorphic controls on hyporheic exchange flow in mountain streams, *Water Resour. Res.*, *39*(1), 1005, doi:10.1029/2002WR001386.
Kessler, A. J., R. N. Glud, M. Bayani Cardenas, M. Larsen, M. F. Bourke, and P. L. M. Cook (2012), Quantifying denitrification in rippled permeable sands through combined flume experiments and modeling, *Limnol. Oceanogr.*, *57*(4), 1217–1232, doi:10.4319/lo.2012.57.4.1217.
Klute, A., and C. Dirksen (1986), Hydraulic conductivity and diffusivity: Laboratory methods, in *Methods of Soil Analysis. Part 1. Physical and Mineralogical Methods, Agron. Monogr. Ser.*, vol. 9, edited by A. Klute, pp. 687–734, Am. Soc. of Agron., Madison, Wis.
Krause, S., C. Tecklenburg, M. Munz, and E. Naden (2013), Streambed nitrogen cycling beyond the hyporheic zone: Flow controls on horizontal patterns and depth distribution of nitrate and dissolved oxygen in the upwelling groundwater of a lowland river, *J. Geophys. Res. Biogeosci.*, *118*, 54–67, doi:10.1029/2012jg002122.
Lewandowski, J., L. Angermann, G. Nützmann, and J. H. Fleckenstein (2011), A heat pulse technique for the determination of small-scale flow directions and flow velocities in the streambed of sand-bed streams, *Hydrol. Processes*, *25*(20), 3244–3255, doi:10.1002/hyp.8062.
Marion, A., M. Bellinello, I. Guymer, and A. Packman (2002), Effect of bed form geometry on the penetration of nonreactive solutes into a streambed, *Water Resour. Res.*, *38*(10), 1209, 27–1–27–12, doi:10.1029/2001WR000264.
Marzadri, A., D. Tonina, and A. Bellin (2012), Morphodynamic controls on redox conditions and on nitrogen dynamics within the hyporheic zone: Application to gravel bed rivers with alternate-bar morphology, *J. Geophys. Res.*, *117*, G00N10, doi:10.1029/2012JG001966.
Mendoza-Lera, C., and M. Mutz (2013), Microbial activity and sediment disturbance modulate the vertical water flux in sandy sediments, *Freshwater Sci.*, *32*(1), 26–38, doi:10.1899/11–165.1.
Mutz, M. (2000), Influences of woody debris on flow patterns and channel morphology in a low energy, sand-bed stream reach, *Intt. Rev. Hydrobiol.*, *85*(1), 107–122.
Mutz, M. (2003), Processes of surface-subsurface water exchange in a low energy sand-bed stream, *Int. Rev. Hydrobiol.*, *88*(3-4), 290–303.
O'Connor, B. L., and M. Hondzo (2008), Enhancement and inhibition of denitrification by fluid-flow and dissolved oxygen flux to stream sediments, *Environ. Sci. Technol.*, *42*(1), 119–125.
O'Connor, B. L. O., and J. W. Harvey (2008), Scaling hyporheic exchange and its influence on biogeochemical reactions in aquatic ecosystems, *Water Resour. Res.*, *44*, W12423, doi:10.1029/2008WR007160.
Packman, A., M. Salehin, and M. Zaramella (2004), Hyporheic exchange with gravel beds: Basic hydrodynamic interactions and bedform-induced advective flows, *J. Hydraul. Eng.*, *130*(7), 647–656, doi:10.1061/(ASCE)0733–9429(2004)130:7(647).
Peterson, E. W., and T. B. Sickbert (2006), Stream water bypass through a meander neck, laterally extending the hyporheic zone, *Hydrogeol. J.*, *14*(8), 1443–1451, doi:10.1007/s10040-006-0050-3.
Ren, J. H., and A. I. Packman (2004), Modeling of simultaneous exchange of colloids and sorbing contaminants between streams and streambeds, *Environ. Sci. Technol.*, *38*(10), 2901–2911.

Ruehl, C. R., A. T. Fisher, M. Los Huertos, S. D. Wankel, C. G. Wheat, C. Kendall, C. E. Hatch, and C. Shennan (2007), Nitrate dynamics within the Pajaro River, a nutrient-rich, losing stream, *J. N. Am. Benthol. Soc.*, *26*(2), 191–206.

Salehin, M., A. I. Packman, and M. Paradis (2004), Hyporheic exchange with heterogeneous streambeds: Laboratory experiments and modeling, *Water Resour. Res.*, *40*, W11504, doi:10.1029/2003WR002567.

Sophocleous, M. (2002), Interactions between groundwater and surface water: the state of the science, *Hydrogeol. J.*, *10*(1), 52–67, doi: 10.1007/s10040-001-0170-8.

Stofleth, J. M., F. D. Shields Jr., and G. A. Fox (2008), Hyporheic and total transient storage in small, sand-bed streams, *Hydrol. Processes*, *1894*, 1885–1894, doi:10.1002/hyp.6773.

Stonedahl, S. H., J. W. Harvey, A. Wörman, M. Salehin, and A. I. Packman (2010), A multiscale model for integrating hyporheic exchange from ripples to meanders, *Water Resour. Res.*, *46*, W12539, doi:10.1029/2009WR008865.

Strommer, J., and L. Smock (1989), Vertical distribution and abundance of invertebrates within the sandy substrate of a low-gradient headwater stream, *Freshwater Biol.*, *22*, 263–274.

Tonina, D., and J. M. Buffington (2007), Hyporheic exchange in gravel bed rivers with pool-riffle morphology: Laboratory experiments and three-dimensional modeling, *Water Resour. Res.*, *43*, W01421, doi:10.1029/2005WR004328.

Trauth, N., C. Schmidt, U. Maier, M. Vieweg, and J. H. Fleckenstein (2013), Coupled 3D stream flow and hyporheic flow model under varying stream and ambient groundwater flow conditions in a pool-riffle system, *Water Resour. Res.*, *49*, 5834–5850, doi:10.1002/wrcr.20442.

Voltz, T., M. Gooseff, A. S. Ward, K. Singha, M. Fitzgerald, and T. Wagener (2013), Riparian hydraulic gradient and stream-groundwater exchange dynamics in steep headwater valleys, *J. Geophys. Res. Earth Surf.*, *118*, 953–969, doi:10.1002/jgrf.20074.

Wondzell, S. M. (2011), The role of the hyporheic zone a stream networks, *Hydrol. Processes*, *25*(22), 3525–3532, doi:10.1002/hyp.8119.

Wörman, A., A. I. Packman, L. Marklund, J. W. Harvey, and S. H. Stone (2007), Fractal topography and subsurface water flows from fluvial bedforms to the continental shield, *Geophys. Res. Lett.*, *34*, L07402, doi:10.1029/2007GL029426.

Zarnetske, J. P., R. Haggerty, S. M. Wondzell, and M. A. Baker (2011), Dynamics of nitrate production and removal as a function of residence time in the hyporheic zone, *J. Geophys. Res.*, *116*, G01025, doi:10.1029/2010JG001356.